Structural features of indoline donors in D-A--A type organic sensitizers for dye-sensitized solar cells

ARTICLE

Structural features of indoline donors in D-A-π-A type organic sensitizers for dye-sensitized solar cells

Received 00th January 20xx,
Accepted 00th January 20xx

DOI: 10.1039/x0xx00000x

Ellie Tanaka,†[a] Maxim S. Mikhailov,†[b] Nikita S. Gudim,[c] Ekaterina A. Knyazeva,[b,c] Ludmila V. Mikhalchenko,[c] Neil Robertson,*[a] and Oleg A. Rakitin*[b,c]

We report three newly synthesized D-A-π-A metal-free organic sensitizers for dye-sensitized solar cells (DSSCs) based on benzo[*c*][1,2,5]thiadiazole as an internal acceptor (A) and N-substituted indolines fused with cyclopentane or cyclohexanes as donor (D) building block. Optical and photovoltaic properties of the new **MAX** series dyes and solar cells based on them were considered in comparison with our previously-reported dye **MAX114** and well-known dye **WS-2**. The effect of replacing the cyclopentane ring with a cyclohexane one, as well as a substituent at the nitrogen atom of the donor fragment (aromatic *p*-tolyl, non-aromatic benzyl and aliphatic 2-ethylhexyl) on the position of absorption maxima in UV/Vis spectra, the E_{HOMO} and E_{LUMO} values of **MAX** series sensitizers and photocurrent density-voltage trends of the corresponding solar cells were studied. It was shown that the **MAX157** dye with a 9-(2-ethylhexyl)-2,3,4,4a,9,9a-hexahydro-1*H*-carbazole donor fragment has a shorter-wavelength absorption maximum in the intra-molecular charge transfer absorption band with the largest molar extinction coefficient in comparison with the other dyes studied. The same dye applied to the TiO_2 surface showed broader optical absorption compared to other dyes in the **MAX** series. All dyes have a relatively narrow HOMO-LUMO gap (1.80-1.90 eV). Amongst the series, DSSCs based on **MAX157** dye recorded the best power conversion efficiency (PCE) of 5.2%, which increased to 5.8% when co-sensitized with **SQ2** dye. All **MAX** dyes reached PCEs varying between 4.4-5.2%, superior to the reference WS-2 dye (3.6%).

1. Introduction

Dye-sensitized solar cells (DSSCs) are one of the most promising complementary technologies to silicon and other inorganic solar energy converters due to their ease of manufacture, mechanical strength, light weight, flexibility, long service life and the ability to work even under reflected and artificial light.[1-4] Organic photosensitizers play a key role in such devices, and substantially determine their performance.[5,6] Modern organic dyes based on individual molecules employ various combinations of the main components: donors (D), acceptors (A), and π-bridges - each of which performs its own important function in finely tuning the photophysical parameters of a substance.[7] Despite the rich variability of structures that can be built from these fragments, their successful use in DSSCs requires a "push-pull" structure, which is dictated by the need to provide intra-molecular charge transfer (ICT) from a donor to an acceptor, which also acts as an anchor.[8,9] Evolution from the simplest D-A type molecules to more complex combinations revealed the most highly-performing structure containing an additional internal acceptor and a π-bridge between the terminal acceptor and donor.[10] The use of D-A-π-A molecules for DSSCs was first proposed by Zhu and co-authors in 2011.[11] One of the most successful dyes described in this work, **WS-2**, was further modified by the authors[6] in order to better understand the effect of individual structural fragments of sensitizers on the properties of final substances. While this work partially shed light on the structure-property relationship, it did not lead to significant improvement of the PCE of solar cells.

In pursuit of improving the photovoltaic characteristics, researchers have followed the path of complicating the chemical structure of dyes, although such complex and cumbersome synthetic sequences have often led to an improvement in PCE by only a fraction of a percent.[12] Such complex dyes are normally obtained from rare and expensive starting compounds by multi-stage synthesis which consists of more than ten stages. As a result, the overall yield of the target substances is prohibitively low. Therefore, it is necessary to continue the search for molecules of the D-A-π-A type, with simpler synthetic schemes, yet providing high photovoltaic parameters.

We have previously established that even a slight change in the structure of the donor fragment has a significant effect on the photovoltaic properties of the final structures.[13] The analogue of **WS-2**, which differs by only one CH_2 group of the donor fragment, **MAX114**, showed a strong hypsochromic shift from 533 nm for **WS-2** to 482 nm for **MAX114**, which confirmed a strong dependence of the ICT band on the donor structure. It is known that the donor fragment plays a significant role in the formation of the energy values

[a] *EaStCHEM School of Chemistry, University of Edinburgh, Edinburgh EH9 3FJ, UK. . Email: neil.robertson@ed.ac.uk.*
[b] *Nanotechnology Education and Research Center, South Ural State University, 454080 Chelyabinsk, Russia.*
[c] *N. D. Zelinsky Institute of Organic Chemistry, Russian Academy of Sciences, 119991 Moscow, Russia. Email: orakitin@ioc.ac.ru.*
† The two authors contributed equally to this work.
Electronic Supplementary Information (ESI) available: detailed characteristics of the DSSCs and spectral characteristics of the synthesized compounds. See DOI: 10.1039/x0xx00000x

of the highest occupied molecular orbital (E_{HOMO}) and for the difference between the energies of the highest occupied and lowest vacant molecular orbital (ΔE or E_{gap}).

Therefore, this work was based on varying the structure of the donor fragment of dyes similar to **WS-2**, using substituents at the nitrogen atom of the indoline ring, as well as the use of a cyclohexane fragment condensed with the latter. This addresses several design features: **MAX140** and **MAX157** with branched alkyl substituents will reduce the area of the dye on the TiO_2 surface; **MAX155** with a benzyl substituent at the indoline nitrogen atom instead of *p*-tolyl will probe whether a conjugated π-system is necessary to adjust the electron-donor properties of fragment D. Furthermore, it will be possible to avoid catalytic arylation of the indoline nitrogen atom, since the alkyl substituents can be introduced by direct N-alkylation, simplifying the synthetic scheme.

2. Results and discussion

2.1. Synthesis and characterization

It was previously shown that structures similar to **WS-2**, although capable of producing high values of current and voltage and, as a consequence, total PCE, suffer from excessive aggregation.[3] In an attempt to avoid this, the authors used a hexyl-substituted π-bridge for the design of the **WS-6** dye, which made it possible to increase the PCE compared to **WS-2** from 5.07% to 6.85%.[12] We have previously shown[13] that replacing the five-membered fused ring in the donor fragment of the **WS-2** sensitizer with a six-membered one also leads to a significant increase in J_{SC} from 11.8 mA cm^{-2} to 14.75 mA cm^{-2}, V_{OC} from 0.59 mV to 0.64 mV, and, as a result, PCE from 5.07%[11] to 5.86%, which is also a consequence of a decrease in aggregation due to the presence of a more bulky cyclohexyl substituent. We continued to study the effect of the introduction of bulky alkyl substituents into the donor part of molecules on the aggregation of dyes on TiO_2 substrates. We chose benzo[*c*][1,2,5]thiadiazole as an internal acceptor, a thiophene ring as a π-bridge, and a cyanoacrylate residue played the role of a terminal acceptor and anchor. The molecular structures of the dyes

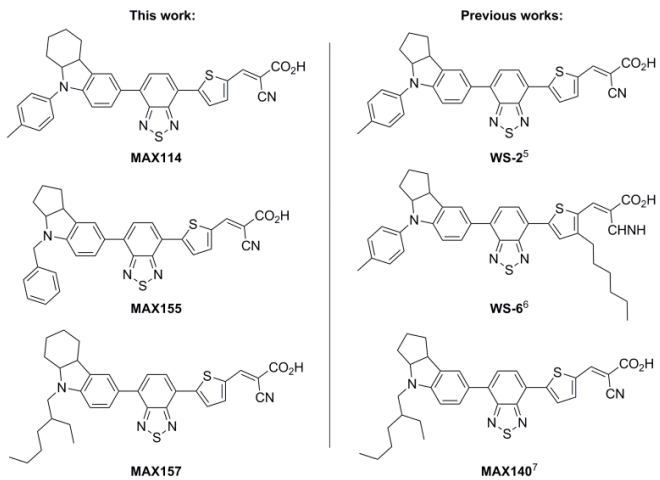

Figure 1. Synthesized and investigated dyes.

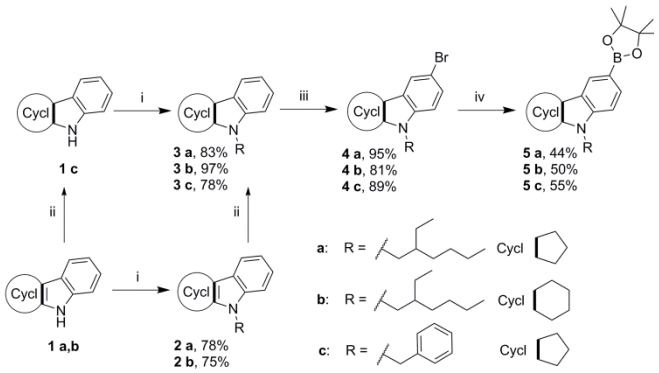

Scheme 1. Synthetic route to **5a-c**: (i) NaH, BnBr or BrC_8H_{17}, DMF; (ii) $NaBH_3CN$, AcOH; (iii) HBr, DMSO, Na_2CO_3, ethyl acetate, (iv) B_2Pin_2, KOAc, $Pd_2(dba)_3$, X-Phos, dioxane.

are shown in Figure 1. The general strategy for the synthesis of dyes with D-A-π-A motif follows a stepwise approach (Schemes 1 and 2).

Initially, the approach to key donor blocks **5** was planned to be carried out similarly to 7- (4,4,5,5-tetramethyl-1,3,2-dioxaborolan-2-yl)-4-(*p*-tolyl)-1,2,3,3a,4,8b-hexahydrocyclopenta[*b*]indole, which was used in the synthesis of the dye **WS-2**,[14] replacing the catalytic arylation step of the indoline nitrogen atom with an alkylation step under nucleophilic substitution reaction conditions. However, it turned out that this approach is applicable only for benzyl derivative **3c**, and 2-ethylhexyl substituted indolines **3a,b** cannot be obtained by this method: alkylation with 1-bromo-2-ethylhexane led to the return of the starting compounds in the case of both indolines **1a,b**. Apparently, the reason lies in the combination of two factors. On the one hand, the geometry of the indoline ring is such that the carbon ring annelated with it partially overlaps the nucleophilic center on the nitrogen atom, making it less capable of attacking sterically loaded substrates. On the other hand, the presence of branching in the immediate vicinity of the reaction center of the attacked bromide imposes an additional steric load and makes the approach of the nucleophile impossible.

We managed to get around this difficulty by changing the synthetic sequence. It turned out that indoles **1a,b** annelated with alicyclic fragments are easily alkylated with sterically hindered 1-bromo-2-ethylhexane under the conditions of a nucleophilic substitution reaction, despite the reduced nucleophilicity of the conjugated nitrogen atom. The alkylated indoles **2a,b** obtained in good yields are reduced under conditions analogous to unsubstituted indoles **1a,b**. Bromination and subsequent replacement of the bromine atom with a protected boronic acid was carried out under the conditions described in the literature earlier (Scheme 1).[14]

Synthesis of the target dyes in the **MAX** and **WS-2** series was carried out using two successive cross-coupling reactions of 4,7-dibromobenzo[*c*][1,2,5]thiadiazole with donor boronic acids **5** and π-spacer **7**. The first stage was carried out under conditions of Suzuki reactions catalyzed by $Pd(PPh_3)_4$ in the presence of aqueous K_2CO_3 in THF to obtain mono-adducts **6a-e** in moderate yields. At the second stage, the conditions of the Stille reaction were used: catalysis by $PdCl_2(PPh_3)_2$ in toluene followed by saponification with HCl to

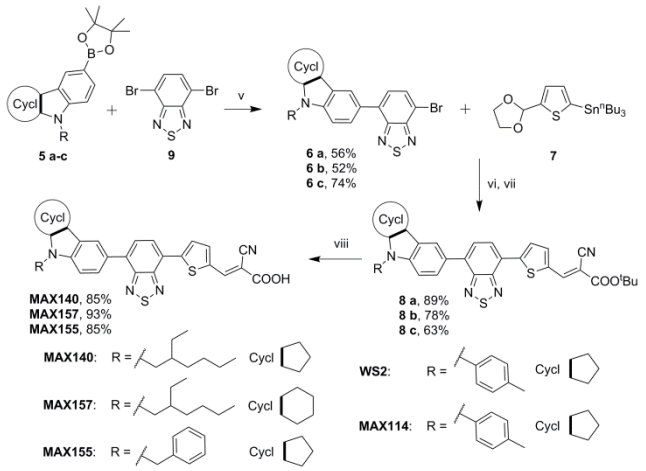

Scheme 2. Synthesis of the target dyes. The reaction conditions: (v) $Pd(PPh_3)_4$, K_2CO_3, dioxane; (vi) $PdCl_2(PPh_3)_2$, toluene, then 2N HCl; (vii) NC-CH_2-COOtBu, NH_4OAc, AcOH, sieve 4Å, toluene; (viii) CF_3COOH, $CHCl_3$.

remove dioxolane protection. The resulting intermediate products were introduced into the Knoevenagel reaction with cyanoacetic acid *tert*-butyl ester without additional isolation and purification. The hydrolysis of esters **8** resulted in the final structures **MAX** and **WS-2**, which, after thorough chromatographic purification (Scheme 2), were used in solar cell device fabrication.

2.2. Optical properties

The UV-Vis optical response of the **MAX** series was recorded in toluene/ethanol (7:3, v/v) at 1 × 10^{-5} M (Fig. 2(a)). The absorption peaks (λ_{max}) and extinction coefficients (ε) are summarized in Table 1. The **MAX** dyes have two marked absorption regions. Short-wavelength absorption maxima in the 390-400 nm range correspond to a π/π* transition, while broad long-wavelength absorption bands in the 505-530 nm range indicate the presence of an intramolecular charge transfer (ICT) process between indoline donor fragments and acceptor groups. The π/π*-transition absorption peak occurs in a narrow range for all dyes studied (the maximum difference is 9 nm), including **WS-2**, which may indicate close values of the energy gap. At the same time, changes in the structure of donor fragments critically affect the intensity of the ICT absorption peaks. Dyes with six-membered annulated cycles **MAX157** and **MAX114** have absorption bands at shorter wavelengths (518 nm and 507 nm, correspondingly) than dyes with cyclopentaindole, and the molar extinction coefficient is almost 2-3 times higher (22.5×$10^3$$M^{-1}$ cm^{-1} for **MAX157** and 20.4×$10^3$$M^{-1}$ cm^{-1} for **MAX114** against 8.83×$10^3$$M^{-1}$ cm^{-1} for **MAX140** and 12.0×$10^3$$M^{-1}$ cm^{-1} for **MAX155**). In this case, the nature of the substituent at the nitrogen atom does not significantly affect the position of the ICT absorption peaks; replacement of the *p*-tolyl substituent with an alkyl substituent leads to a slight red shift of the absorption maxima for cyclopentaindoline derivatives (from 533 nm for **WS-2** to 541 nm for **MAX140**) and for cyclohexaindoline dyes (from 507 nm for **MAX114** to 518 nm for **MAX157**). This may mean that there is no significant contribution of *p*-tolyl substituents of the **WS-2** and **MAX114** dyes to the general conjugation system; therefore, replacing aryl substituents with alkyl substituents will not worsen the optical properties of sensitizers.

The absorption spectra of all dyes including **WS-2** loaded on TiO_2 are shown in Fig. 2(b). The overall profiles differ from those in solution. All dyes show hypsochromic shifts, but the effect is negligible, resulting in an absorption profile that sits in the visible range. Nevertheless, the presence of a blue shift of the absorption peaks on TiO_2 compared with that in solution proves the absorption of the dye on the TiO_2 surface through the deprotonation of the carboxylic group and suggests the formation of *H*-aggregates characteristic of dyes, with good planarity and the possibility of parallel arrangement. **MAX140** and **MAX157** show broader optical absorption compared to **MAX114** and **MAX155**, suggesting the higher light harvesting ability of these two dyes.

Table 1. UV-Vis absorption characteristics of the **MAX** series

Dye	λ_{max1}/nm[a] (ε_{max1}×$10^3$$M^{-1}$ cm^{-1})	λ_{max2}/nm[a] (ε_{max2}×$10^3$$M^{-1}$ cm^{-1})	$\lambda_{max,\ film}$/nm[b]
MAX114	392 (16.3)	507 (20.4)	466
MAX140	401 (7.48)	541 (8.83)	478
MAX155	398 (9.83)	530 (12.0)	466
MAX157	397 (18.1)	518 (22.5)	486
WS-2	394[c] (14.1)[c]	533[c] (16.7)[c]	492

[a]The UV-Vis optical responses were obtained in toluene/ethanol (7:3, v/v) solution.[b] The dyes were absorbed on TiO_2 film. [c]These values were taken from the literature.[5]

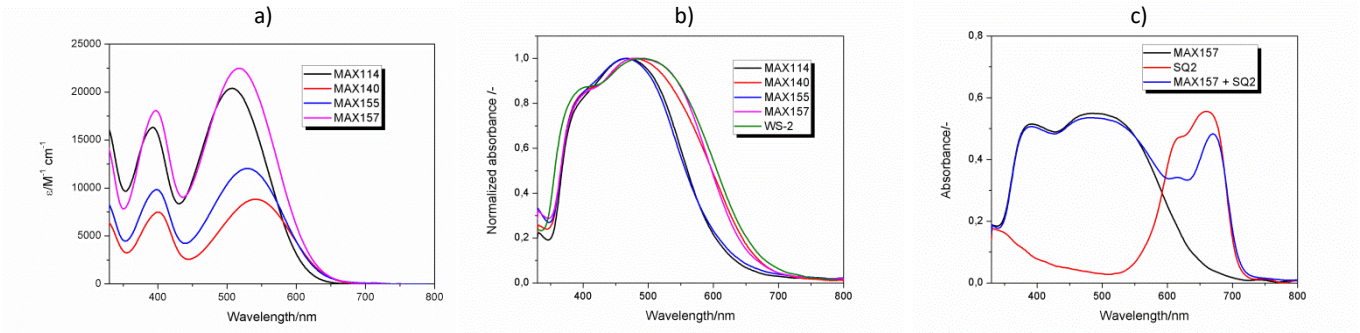

Fig. 2. UV-Vis absorption of (a) **MAX** series in toluene/ethanol (7:3, v/v) at 1×10^{-5} M, (b) **MAX** series adsorbed on transparent TiO_2 film, and (c) **MAX157** and **SQ2** co-adsorbed on transparent TiO_2 film along with **MAX157** and **SQ2** independently adsorbed on TiO_2 film

MAX157, which has the highest molecular extinction coefficient and broadest UV-Vis absorption range, was co-sensitized with the squaraine **SQ2** dye as in Fig. 2(c). The co-sensitized **MAX157** + **SQ2** clearly displays the spectrum closest to panchromatic in respect to the mono-sensitized films.

2.3. Electrochemical properties

To estimate the energy values of the frontier orbitals, the values of the peak potentials of the electrooxidation (EO) and electroreduction (ER) of the **MAX** compounds obtained by cyclic voltammetry were used. The studied compounds have similar peak potentials of ER and EO (Fig. 3). The first stages of their ER are reversible at the potential sweep rate v = 0.1 Vs^{-1}. The EO peaks become quasi-reversible with an increase in v ≥ 1 Vs^{-1}. The oxidation peak of **MAX114** is irreversible up to v = 10 Vs^{-1}.

The energies of the lowest unoccupied molecular orbital (LUMO) and the highest occupied molecular orbital (HOMO) were estimated from the values of the formal reduction $E^{red} = (E_{pc}+E_{pa})/2$ and oxidation $E^{ox}=(E_{pa}+E_{pc})/2$ potentials, respectively. The values of $E^{red}{}_{Fc\,/\,Fc+}$ and $E^{ox}{}_{Fc/Fc+}$ were calculated relative to the potential of the reversible ferrocene/ferrocenium (Fc/Fc+) redox pair (Table 2), taking into account that the absolute oxidation potential of ferrocene is -5.1 eV.[15,16] These values were used to calculate the values of the LUMO and HOMO using the formulas:

$$E_{HOMO}\,(eV) = -\,|e|(E^{ox}{}_{Fc/Fc+} + 5.1) \qquad (1)$$

$$E_{LUMO}\,(eV) = -\,|e|(E^{red}{}_{,\,Fc/Fc+} + 5.1) \qquad (2)$$

The obtained LUMO values of the compounds are higher than the TiO_2 semiconductor energy level (-4.2 eV),[17] and the HOMO values are lower than the I^-/I_3^- (-5.2 eV) level.[18] These parameters confirm the suitability of the **MAX** compounds as dye candidates in DSSCs. The relatively narrow HOMO-LUMO gaps of the **MAX** series, where **MAX114** (1.91 eV) > **MAX155** (1.88 eV) > **MAX157** (1.84 eV) > **MAX140** (1.80 eV), suggest that a higher current density could be achieved in the solar cell.[19]

2.4. DSSC performance

2.4.1. Photovoltaic performance of the MAX series. The novel dyes, **MAX140**, **MAX155** and **MAX157**, were tested in DSSCs with the I^-/I_3^- electrolyte under AM1.5G irradiation in comparison with the reference **WS-2** dye and previously reported **MAX114** dye. First of all, the incident photon to current efficiency (IPCE) of one batch of all MAX dyes were recorded as in Fig. S1, to confirm the validity of the IV tests hereon. Indeed, the simulated current density is shown to approximate the current density obtained from the IV measurements. The photovoltaic characteristics of the best devices obtained for each dye are summarized in Table 3, and the corresponding *J-V* curves are presented in Fig. 4. The statistics are shown in the ESI (Table S1). Remarkably, all **MAX** dyes exhibited superior performance to the reference **WS-2** dye (3.6%), reaching 4.94%, 5.15%, 4.38% and 5.20% for **MAX114**, **MAX140**, **MAX155** and **MAX157**, respectively. The improvements are attributed to the increased current and voltage in the cells. Amongst the series, two dyes **MAX140** and **MAX157** with 2-ethylhexyl alkyl chain in the donor part present the highest PCEs over 5% and J_{SC} values of 13.87 mA·cm^{-2} and 12.02 mA·cm^{-2}, respectively. The higher performance of these dyes can be attributed to the broader optical absorption which will improve the light harvesting. The DSSCs based on **MAX157** dye have a maximum V_{OC} value, which may indicate more pronounced electron-recombination blocking of 9-(2-ethylhexyl)-2,3,4,4a,9,9a-hexahydro-1*H*-carbazol-6-yl moiety in comparison with the other donors. Indeed, electrochemical impedance spectroscopy (EIS) (Fig. S2) reveals that the electron lifetime and recombination resistance are higher for **MAX 157** within the series. On the other hand, the low

Table 2. Electrochemical properties of the **MAX** series in DMF

Dye	E^{red} (*vs* Fc/Fc$^+$)^a, V	$E_{LUMO}{}^b$, eV	E^{ox} (*vs* Fc/Fc$^+$)^a, V	$E_{HOMO}{}^b$, eV	$E_g{}^c$, eV
MAX114	-1.62	-3.48	0.29^d	-5.39	1.91
MAX140	-1.60	-3.50	0.20	-5.30	1.80
MAX155	-1.62	-3.48	0.26	-5.36	1.88
MAX157	-1.61	-3.49	0.23	-5.33	1.84

^{a}Here $E^{ox}=(E_{pa}+E_{pc})/2$ and $E^{red} = (E_{pc}+E_{pa})/2$ are oxidation and reduction potential relative to Fc/Fc$^+$ respectively. ^{b}Energies of frontier orbitals were calculated according to equations (1) and (2). ^{c}Eg= E_{LUMO} -E_{HOMO}. ^{d} The potential E_{pa} of the irreversible oxidation peak is given.

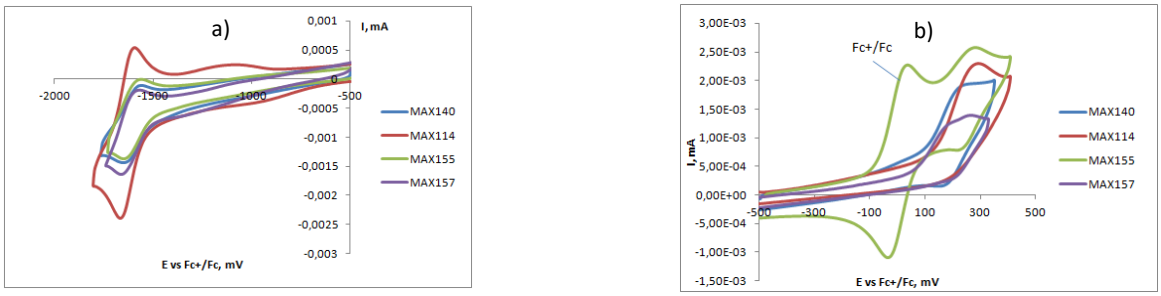

Fig. 3. CV curves reduction (a) and oxidation (b) of the **MAX** series in DMF solutions (0.1 M Bu_4NClO_4, Pt-electrode, 0.1 Vs^{-1})

chemical capacitance for the **MAX** dyes compared to **N719** leads to a shorter electron lifetime range, which explains the relatively low V_{OC} range below 0.6 V.

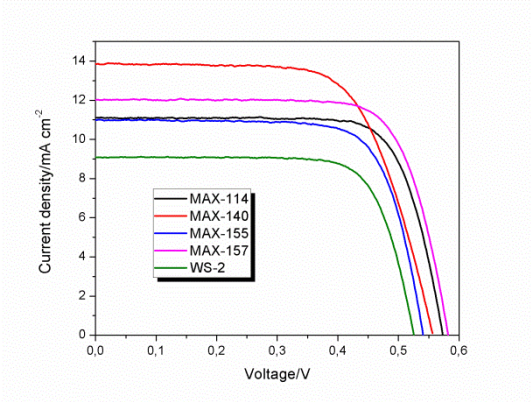

Fig. 4. Current density–voltage curves of the best DSSCs using the **MAX** dyes and **WS-2** dye at AM1.5G, 100 mW cm^{-2} with 4 µm transparent TiO_2 layer and CDCA additions

The full set of the **MAX** dyes were tested in DSSCs with a transparent TiO_2 film thickness of 4 µm, since it was shown using the **MAX140** dye as an example (see Table S2, Fig. S3 in ESI) that an increase in the transparent layer thickness to 8 and 12 µm leads to a decrease in J_{SC} (to 11.96 and 11.58 mA cm^{-2}, respectively), V_{OC} (up to 0.54 and 0.52 mV, respectively) and PCE (up to 4.71 and 4.15%, respectively) values, which is probably associated with the occurrence of dye aggregation due to increasing the dye loading amount. In addition, a thinner TiO_2 layer minimizes charge-transport losses.[20]

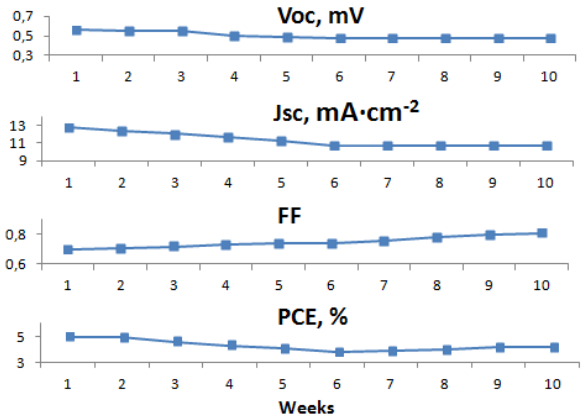

Fig. 5. The photovoltaic parameters (V_{OC}, J_{SC}, FF, and PCE) variation with aging time for the **MAX140** solar devices

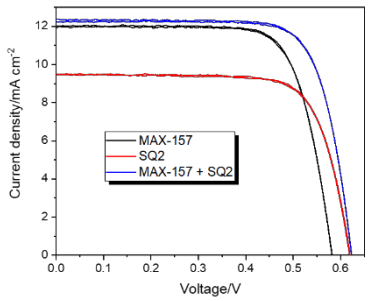

Fig. 6. Current density–voltage curves of the best **MAX157**, **SQ2** and **MAX157** + **SQ2** sensitized DSSCs at AM1.5G, 100 mW cm^{-2} with 4 µm transparent TiO_2 layer and CDCA additions

Table 3. DSSC characteristics for the best devices using the **MAX** series[a]

Dye	J_{SC}/mA·cm^{-2}	V_{OC}/mV	*FF*	PCE (%)
MAX114	11.51	0.57	0.75	4.94
MAX140	13.87	0.56	0.66	5.15
MAX155	10.99	0.54	0.74	4.38
MAX157	12.02	0.58	0.75	5.20
WS-2	9.10	0.52	0.75	3.57

To achieve the maximum photovoltaic parameters, the chenodeoxycholic acid (CDCA) additive turned out to be beneficial, analogous to previous reports claiming that it prevents excessive dye aggregation. The DSSC performance based on **MAX140** without any addition of CDCA (J_{SC} = 7.17 mA·cm^{-2}, V_{OC} = 0.51 mV, PCE = 2.68%, see Table S3, Fig. S4 in ESI) is almost twice lower than with the addition of CDCA.

Thus, DSSCs based on the three dyes we prepared showed better results compared to the reference dye **WS-2**. To assess the possible use of the new dyes in practice, it is necessary to understand how stable the devices are under normal operating conditions. The most vulnerable link that can significantly shorten the lifespan of DSSCs is the dye, which can irreversibly degrade with prolonged exposure to sunlight. The change in photovoltaic characteristics with time when exposed to sunlight is direct evidence of the stability of the photosensitizer.

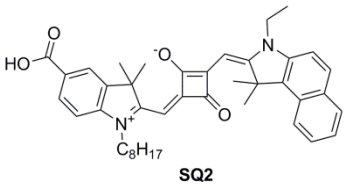

SQ2

Fig. 7. The chemical structure of co-sensitizer **SQ2**

Using the **MAX140** dye as an example, it was shown that during normal operation within five weeks there is a gradual decrease in photovoltaic parameters (Table S4, Fig. S5 in ESI), and the PCE value decreases by almost 15%. Fig. 5 shows the evolution of the basic parameters (J_{SC}, V_{OC}, FF, and PCE) of a **MAX140** solar cell over time when kept under normal operating conditions (in the dark at night and under direct or scattered sunlight during the day). From the above dependences it can be seen that after ten weeks (a total of *ca*. 1680 h, which corresponds to 840 h under normal sunlight), there is

Table 4. Photovoltaic parameters for DSSCs based on **MAX157**, **SQ2**, and **MAX157 + SQ2** (cosensitization)

Dye	J_{SC}/mA·cm^{-2}	V_{OC}/mV	*FF*	PCE (%)
MAX157	12.02	0.58	0.75	5.20
SQ2	9.48	0.62	0.75	4.39
MAX157 + SQ2	12.38	0.62	0.76	5.80

only a slight decrease in the photocurrent value, fill factor and, as a consequence, PCE, which indicates that the whole the system reaches equilibrium and further changes are minor.

2.4.2. Co-sensitizing MAX157 with SQ2. Co-sensitization is a powerful technique to further broaden the absorption spectra of the original dye.[21] In this regard, **MAX157**, the best performing dye in the **MAX** series, was co-sensitized with a well-known squaraine blue dye **SQ2** (Fig. 7),[22] absorbing in near-infrared region. The UV-Vis absorption profile in Fig. 2(c) shows the complementary effect of both dyes in the co-sensitized cell, expanding the light-harvesting region. Thanks to the use of **SQ2** as a co-sensitizer agent for **MAX157**, it was possible to effectively cover the region from 300 to 700 nm without reducing the absorbance during co-absorption on transparent TiO_2 film.

As a result, a slight shift in current and a clear improvement in voltage were observed for **MAX157** & **SQ2**-sensitized solar cells as shown in Table 4 and Fig. 6. The J_{SC} value upon cosensitization with **SQ2** was able to increase from 12.02 mA cm^{-2} to 12.38 mA cm^{-2}, while the V_{OC} value - from 0.58 mV to 0.62 mV, suggesting better blocking of recombination of electrons in the titania with the electrolyte. The overall efficiency for cosensitization was 10% higher, from 5.20% for the individual **MAX157** dye to 5.80% when using the co-sensitized system.

3. Experimental details

3.1. Materials and reagents

The reagents were purchased from commercial sources and used as received. 1,2,3,4-Tetrahydrocyclopenta[*b*]indole **1a**,[23] 2,3,4,9-tetrahydro-1*H*-carbazole **1b**,[24] 1,2,3,3a,4,8b-hexahydrocyclopenta[*b*]indole **1c**,[25] 4-(*p*-tolyl)-7-(4,4,5,5-tetramethyl-1,3,2-dioxaborolan-2-yl)-1,2,3,3a,4,8b-hexahydrocyclopenta[*b*]indole **5d**,[14] 9-(*p*-tolyl)-6-(4,4,5,5-tetramethyl-1,3,2-dioxaborolan-2-yl)-2,3,4,4a,9,9a-hexahydro-1*H*-carbazole **5e**,[13] (5-(1,3-dioxolan-2-yl)thiophen-2-yl)tributylstannane 7,[26] 4,7-dibromobenzo[*c*][1,2,5]thiadiazole **9**,[27] 2-cyano-3-(5-(7-(9-(*p*-tolyl)-2,3,4,4a,9,9a-hexahydro-1*H*-carbazol-6-yl)benzo[*c*][1,2,5]thiadiazol-4-yl)thiophen-2-yl)acrylic acid **MAX114**,[7] and 2-cyano-3-(5-(7-(4-(*p*-tolyl)-1,2,3,3a,4,8b-hexahydrocyclopenta[*b*]indol-7-yl)benzo[*c*][1,2,5]thiadiazol-4-yl)thiophen-2-yl)acrylic acid **WS-2**[11] were prepared according to the published methods and characterized by NMR spectra. All synthetic operations were performed under a dry argon atmosphere. Solvents were purified by distillation from the appropriate drying agents.

3.2. Analytical instruments

Elemental analyses were recorded on Elemental Analyser Perkin Elmer 2400. Melting points are uncorrected and were obtained by a Kofler hot-stage apparatus. ^{1}H NMR (300.1 MHz) and ^{13}C NMR (75.5 MHz) spectra were obtained by a Bruker AM-300 spectrometer with TMS as the standard in DMSO-d_6 or $CDCl_3$ solutions. The coupling constant (*J*) values are reported in Hertz (Hz). MS spectra were taken with a Finnigan MAT INCOS 50 instrument (EI, 70 eV). High-resolution MS spectra were recorded on a Bruker micrOTOF II instrument with ionization by electrospray (ESI). The measurement was operated in a negative ion mode (3200 V) or in a positive ion mode (interface capillary voltage –4500 V); mass range: m/z 50 - 3000 Da; internal or external calibration was made with Electrospray Calibrant Solution (Fluka). For solutions in methanol, water, or acetonitrile a syringe injection was used (flow rate 3 mL·min^{-1}). As a dry gas nitrogen was applied; interface temperature - 180°C. IR spectra were recorded in KBr pellets on a Specord M-80 instrument.

3.3. General procedure for fabrication and characterization of DSSCs

Clean fluorine doped tin oxide (FTO) conductive glass substrates (7 Ω/□, 2.2 mm-thick, TCO22-7/LI, Solaronix) were treated with 40 mM $TiCl_4$ aqueous solution at 80 °C for 30 min on a hotplate. Transparent and scattering TiO_2 pastes (18NR-T and 18NR-AO, then Greatcell Solar, now Greatcell Solar Materials) were deposited on the treated substrates, one layer each, by screen printing. The TiO_2 electrodes were annealed in a furnace at 325 °C for 5 °C min, 375 °C for 5 min, 450 °C for 15 min and 500 °C for 15 min (ramp: 10 °C/min), resulting in ~8 µm-thick (4 µm + 4 µm) mesoporous TiO_2 films. The films were treated for a second time in $TiCl_4$ solution, followed by annealing at 500 °C for 30 min. The electrodes were immersed in the dye bath while still warm (~80 °C). The dye baths consisted of 0.5 mM in ethanol with 5 mM chenodeoxycholic acid (CDCA) for **MAX140** and **MAX157**, 0.5 mM in toluene/ethanol (7:3, v/v) with 5 mM CDCA for **MAX114** and **MAX155**, 0.3 mM in acetonitrile and *n*-butanol (85:15, v/v) with 3 mM CDCA for **SQ2**, and 0.3 mM in chloroform with 20 mM CDCA for **WS-2**. A 'dye-cocktail' was prepared for the co-sensitization of **MAX157** and **SQ2**, by mixing the aforementioned dye baths for each dye at a 1:1 ratio. The dye adsorption was performed overnight. For the counter electrodes, a platinum precursor paste (Platisol T, Solaronix) was doctor-bladed on clean FTO glass substrates and fired at 450 °C for 10 minutes. The anode and cathode were assembled with a 25 µm-thick thermoplastic gasket (Surlyn, DuPont), and the electrolyte was injected under vacuum through a predrilled hole in the cathode. The electrolyte in our study consisted of 0.6 M 1,2-dimethyl-3-propylimidazolium iodide, 0.1 M LiI, 0.05 M iodine and 0.5 M 4-*tert*-butylpyridine in anhydrous acetonitrile.

Current-voltage (*J-V*) characteristics were recorded on a potentiostat (Autolab, Metrohm) equipped with AM1.5G (100 mW cm^{-2}) simulated sunlight as light source, generated by a class AAA solar simulator (SLB300A, Sciencetech). The intensity of the incident light was calibrated with a Si reference cell. The active area of the solar cell was fixed to 0.0625 cm^2 by a black metal mask.

The incident photon-to-current conversion efficiency (IPCE) was recorded on a Bentham PVE300 EQE/IQE system in DC mode. The incident light was calibrated with a Si reference photodiode.

Electrochemical impedance spectroscopy (EIS) measurements were performed using a similar setup to the *J-V* measurements. The signal was recorded with an Autolab potentiostat, where the AC voltage was set to an amplitude of 10mV and the frequency was ranged from 0.1 Hz to 100 kHz. The DSSCs were tested at *Voc* under AM1.5G illumination.

3.4. Optical characterization

The UV-Vis absorption spectra were recorded at room temperature on a Jasco V-670 UV/Vis/NIR spectrophotometer controlled with SpectraManager software. The solution UV-Vis samples were prepared as 1×10^{-5} M toluene/ethanol (7:3, v/v) solutions in a 1 cm quartz cell. Solid UV-Vis samples were prepared by adsorbing the dyes onto 4 µm-thick transparent TiO_2 films on FTO glass. The reference was blank FTO glass.

3.5. Electrochemical measurements

Cyclic voltammograms were recorded using an IPC-Pro potentiostat (Econix, Russia) according to a three-electron scheme. A 0.1 M solution of Bu_4NBF_4 in DMF was used as the background electrolyte. The working electrode was a platinum electrode, the counter electrode was a platinum grid, and the reference electrode was a saturated calomel electrode connected to the solution in the cell via a bridge filled with a background electrolyte. The potentials were determined relative to the reversible oxidation potential of ferrocene added to the solution after registering the curves of the studied compounds. The solution was purged with high-purity argon to remove dissolved oxygen. The curves were recorded at a potential sweep rate of 0.1-10.0 Vs^{-1}.

3.6. General procedure for alkylation of indoles 1a-c.

The mixture of 15ml DMF and indole **1a-c** (17.3 mmol) was stirred for 5 min at 0°C then NaH (1.1 g, 60% suspension in mineral oil, 34.6 mmol) was added and the mixture was stirred at room temperature for 1 h and cooled to 0°C. 1-Bromo-2-ethylhexane (for **1a,b**), or benzyl bromide (for **1c**) (26 mmol) was added dropwise at 0°C. Then, the mixture was stirred for another 30 min at room temperature, poured into cold water, washed with ethyl acetate (3 × 50 ml). The combined organic phases were dried over $MgSO_4$, filtered, and evaporated under reduced pressure. The crude product was purified on a silica gel column with petroleum ether.

3.7. General procedure for hydration of indole derivatives 2a,b.

The solution of sodium cyanoborohydride (1.7 g, 27 mmol) in 25 ml of acetic acid was added dropwise to a solution of indole **2a,b** (13.5 mmol) in 15 ml of acetic acid at stirring at room temperature. The reaction mixture is stirred for 20 hours and then diluted with water (75 ml) and extracted with ethyl acetate (3 × 50 ml). The combined organic phases were washed with a sodium carbonate solution (3 × 50 ml), dried over $MgSO_4$, filtered, and evaporated under reduced pressure. The residue is purified by silica column chromatography with petroleum ether.

3.8. General procedure for bromination of indoline derivatives 3.

To a solution of **3** (11 mmol) and DMSO (0.86 ml, 12.2 mmol) in ethyl acetate (25 ml) hydrobromic acid (48%, 3 ml, 24.5 mmol) was added dropwise at 60 °C. After 5 min K_2CO_3 (1.6 g) was added and the mixture was stirred another 1 h. After cooling down to room temperature the mixture was diluted with ethyl acetate (50 ml) and washed with water (3 × 50 ml). The combined organic phases were dried over $MgSO_4$, filtered, and evaporated under reduced pressure. The residue is purified by silica column chromatography with petroleum ether.

3.9. General procedure for borylation reaction of compounds 4.

The solution of compound **4** (4.28 mmol), B_2Pin_2 (1.6 g, 6.4 mmol), and potassium acetate (1.5 g, 15.3 mmol) were dissolved in dioxane (25 ml), degassed for 20 minutes with a stream of argon, and $Pd_2(dba)_3$ (39 mg, 0.04 mmol) and X-Phos (81 mg, 0.17 mmol) were added simultaneously. The reaction was then stirred at 80°C for 20 h, and then diluted with ethyl acetate (25 ml) and plugged through a thin pad of celite. The mixture was evaporated and the residue was purified by silica column chromatography with ethyl acetate/petroleum ether 1:50.

3.10. General procedure for the cross-coupling of 4,7-dibromobenzo[*c*][1,2,5]tiadiazoles and boronic ester 5.

Boronic ether **5** (1.76 mmol) and 4,7-dibromobenzo[*c*][1,2,5]-tiadiazole **9** (518 mg, 1.76 mmol) were dissolved in dioxane (20 ml), and 2M solution of K_2CO_3 (15 ml) was added. The mixture was degassed for 20 min with a stream of argon at stirring, and $Pd(PPh_3)_4$ (98 mg, 88 µmol, 5 mol %) was added. After refluxing for 10 h, the mixture was diluted with water (25 ml) and extracted with ethyl acetate (3 × 25 ml). The combined organic phases were washed with a sodium carbonate solution (3 × 50 ml), dried over $MgSO_4$, filtered, and evaporated under reduced pressure. The residue was purified by silica column chromatography with ethyl acetate/petroleum ether 1:25.

3.11. General procedure for the cross-coupling and subsequent Knoevenagel reactions of mono-adducts 6.

Compounds **6** (0.83 mmol) and **7** (550 mg, 1.24 mmol) were dissolved in toluene (20 ml). The mixture was degassed for 20 minutes with a stream of argon at stirring, and $PdCl_2(PPh_3)_2$ (50 mg, 0,043 mmol) was added. After refluxing for 6 h, the reaction mixture was treated with 2N HCl (20 ml) for 1h, washed with water (3 × 25 ml), organic phase was dried over $MgSO_4$, filtered, and concentrated under reduced pressure. The residue was purified by flash chromatography with ethyl acetate. The product was used in the next step without further purification. The crude product was dissolved in toluene (20 ml), the cyanoacetic acid *tert*-butyl ester (175 mg, 1.24 mmol), ammonium acetate (100 mg, 1.30 mmol) and acetic acid (1 ml) were added, and the mixture was refluxed with molecular sieve 4Å for 2 h. After refluxing, the reaction mixture was diluted with water (25 ml) and extracted with ethyl acetate (3 × 25 ml). The combined organic phases were washed with a sodium carbonate solution (3 × 50 ml), dried over $MgSO_4$, filtered, and evaporated under reduced pressure. The residue is purified by silica column chromatography with ethyl acetate/petroleum ether 1:20.

3.12. General procedure for hydrolyses of ethers 8.

Compound **8** (0.045 mmol) was dissolved in solution of $CF_3COOH/CHCl_3$ (5 ml, 1:3). After stirring for 5 h under argon at room temperature, the mixture was diluted with dichloromethane (25 ml), and washed with water (3 × 25 ml). The combined organic phases were dried over $MgSO_4$, filtered, and evaporated under reduced pressure. The residue is purified by silica column chromatography with ethyl acetate/petroleum ether methanol/dichloromethane 1:5.

4. Conclusions

In summary, three novel organic D-A-π-A dyes were synthesized from which the DSSCs were constructed. *N*-substituted indolines fused with cyclopentane or cyclohexanes were considered as donor fragments, and the influence of individual structural fragments on the optical and photovoltaic properties of new dyes was established. It turned out that regardless of the structure of the donor part, all dyes have a relatively narrow energy gap, and the position of E_{HOMO} and E_{LUMO} is suitable for the effective use of these dyes in solar cells. Taking **MAX140** as an example, DSSCs employing the MAX series were found to be relatively stable under normal operating conditions for 10 weeks. It was shown that, in the case of derivatives 2,3,4,4a,9,9a-hexahydro-1*H*-carbazole, replacement of the *p*-tolyl substituent at the N atom (dye **MAX114**) by 2-ethylhexyl (dye **MAX157**) leads to a short-wavelength shift of the absorption maximum in the ICT band and an increase in the molar extinction coefficient. Solar cells based on this dye showed a maximum efficiency of 5.2%, which was increased to 5.8% using the co-sensitization technique with **SQ2** dye as co-sensitizer. Thus, we have shown that even a slight change in the structure of individual structural fragments of D-A-π-A dyes has a significant effect on the optical and photovoltaic properties, which is often impossible to predict based on existing theories.

Author Contributions

Investigation and writing – review & editing, E.T.; investigation, M.S.M., N.S.G., L.V.M.; investigation and writing – original draft, E.A.K., methodology and conceptualization, N.R.; validation and conceptualization, O.A.R.

Conflicts of interest

There are no conflicts to declare.

Acknowledgements

The authors gratefully acknowledge the financial support of the Russian Foundation for Basic Research (project 20-43-740003). The authors thank the Centre for Plastic Electronics for access to the IPCE facility. Ellie Tanaka is grateful to the Japan Student Services Organization for a PhD studentship.

Notes and references

1 B. O'Regan, M. Grätzel, *Nature,* 1991, **353**, 737.
2 A. Mishra, Markus K. R. Fischer, P. Bäuerle, *Angew. Chem. Int. Ed*. 2009, **48**, 2474.
3 Y. Wu, W. Zhu, *Chem. Soc. Rev.,* 2013, **42**, 2039.
4 E. A. Knyazeva, O. A. Rakitin, *Russ. Chem. Rev*., 2016, ***85***, 1146.
5 A. Carella, F. Borbone, R. Centore, *Front. Chem*., 2018, **8**, 00481.
6 H. Jiang, Y. Wu, A. Islam, M. Wu, W. Zhang, C. Shen, H. Zhang, E. Li, H. Tian, W.-H. Zhu, *ACS Appl. Mater. Interfaces*, 2018, **10**, 13635.
7 T. C. Parker, D. G. (Dan) Patel, K. Moudgil, S. Barlow, C. Risko, J.-L. Brédas, J. R. Reynolds, S. R. Marder, *Mater. Horiz*., 2015, **2**, 22.
8 T.-D. Kim, K.-S. Lee, *Macromol. Rapid Commun*., 2015*,* **36***,* 943.
9 Y. Wu, W.-H. Zhu, S. M. Zakeeruddin, M. Grätzel, *ACS Appl. Mater. Interfaces*, 2015, **7**, 9307.
10 S. Chaurasia, J. T. Lin, *Chem. Rec*., 2016, **16**, 1311.
11 W. Zhu, Y. Wu, S. Wang, W. Li, X. Li, J. Chen, Z.-s. Wang, H. Tian, *Adv. Funct. Mater*., 2011, **21**, 756.
12 Y. Wu, X. Zhang, W. Li, Z.-S. Wang, H. Tian, W. Zhu, *Adv. Energy Mater*., 2012, **2**, 149.
13 M. S. Mikhailov, N. S. Gudim, E. A. Knyazeva, E. Tanaka, L. Zhang, L. V. Mikhalchenko, N. Robertson, O. A. Rakitin, *J. Photochem. Photobiol. A,* 2020, **391**, 112333.
14 Md. Akhtaruzzaman, Y. Seya, N. Asao, A. Islam, E. Kwon, A. El-Shafei, L. Hanc, Y. Yamamoto, *J. Mater. Chem*., 2012, **22**, 10771.
15 C. M. Cardona, W. Li, A. E. Kaifer, D. Stockdale, G. C. Bazan, *Adv. Mater*., 2011, **23**, 2367.
16 P. Bujak, I. Kulszewicz-Bajer, M. Zagorska, V. Maurel, I. Wielgusa, A. Pron, *Chem. Soc. Rev*., 2013, **42**, 8895.
17 G. Oskam, B. V. Bergeron, G. J. Meyer, P. C. Searson, *J. Phys. Chem. B,* 2001, **105**, 6867.
18 D. D. Babu, H. Cheema, D. Elsherbiny, A. El-Shafei, A. V. Adhikari, *Electrochim. Acta,* 2015, **176**, 868.
19 A. V. Akkuratov, P. A. Troshin, *Polym. Sci., Ser. B,* 2014, **56**, 414
20 G. D. Sharma, M. S. Roy, S. P. Singh, *J. Mater. Chem*., 2012, **22**, 18788.
21 J. M. Cole, G. Pepe, O. K. Al Bahri, C. B. Cooper, *Chem. Rev*., 2019, **119**, 7279
22 T. Geiger, S. Kuster, J.-H. Yum, S.-J. Moon, M. K. Nazeeruddin, M. Grätzel, F. Nüesch, *Adv. Funct. Mater*., 2009, **19**, 2720.
23 G. S. Welmakera, J. E. Sabalski, *Tetrahedron Lett*., 2004, **45**, 4851.
24 G. D. Sharma, M. S. Roy, S. P. Singh, *J. Mater. Chem*., 2012, **22**, 18788.
25 Y. Wang, Z. Zheng, T. Li, N. Robertson, H. Xiang, W. Wu, J. Hua, W.-H. Zhu, H. Tian, *ACS Appl. Mater. Interfaces* 2016, **8**, 31016.
26 D. Prim, A. Auffrant, Z. F. Plyta, J.-P. Tranchier, F. Rose-Munch, E. Rose, *J. Organomet. Chem*., 2001, **624**, 124.
27 K. Pilgram, M. Zupan, *J. Heterocycl. Chem*., 1970, **7**, 629.

